

Article

Induction of Intracellular Ca^{2+} and pH Changes in Sf9 Insect Cells by Rhodojaponin-III, A Natural Botanic Insecticide Isolated from *Rhododendron molle*

Xing-An Cheng, Jian-Jun Xie, Mei-Ying Hu *, Yan-Bo Zhang and Jing-Fei Huang

Laboratory of Insect Toxicology, South China Agricultural University, Guangzhou 510642, China; E-Mails: anzai_28@163.com (X.-A.C); 245738742@qq.com (J.-J.X); fiend_wing_bo@yahoo.com.cn (Y.-B.Z); huangjingfei@163.com (J.-F.H)

* Author to whom correspondence should be addressed; E-Mail: humy@scau.edu.cn; Tel.: +86-20-8528-0308, Fax: +86-20-8528-0292.

Received: 25 January 2011; in revised form; 6 April 2011 / Accepted: 7 April 2011 /

Published: 15 April 2011

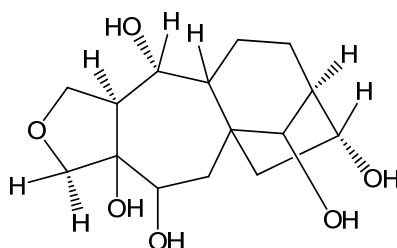
Abstract: Many studies on intracellular calcium ($[\text{Ca}^{2+}]_i$) and intracellular pH (pH_i) have been carried out due to their importance in regulation of different cellular functions. However, most of the previous studies are focused on human or mammalian cells. The purpose of the present study was to characterize the effect of Rhodojaponin-III (R-III) on $[\text{Ca}^{2+}]_i$ and pH_i and the proliferation of Sf9 cells. R-III strongly inhibited Sf9 cells proliferation with a time- and dose-dependent manner. Flow cytometry established that R-III interfered with Sf9 cells division and arrested them in G2/M. By using confocal scanning technique, effects of R-III on intracellular free calcium ($[\text{Ca}^{2+}]_i$) and intracellular pH (pH_i) in Sf9 cells were determined. R-III induced a significant dose-dependent (1, 10, 100, 200 $\mu\text{g}/\text{mL}$) increase in $[\text{Ca}^{2+}]_i$ and pH_i of Sf9 cells in presence of Ca^{2+} -containing solution (Hanks) and an irreversible decrease in the absence of extra cellular Ca^{2+} . We also found that both extra cellular Ca^{2+} and intracellular Ca^{2+} stores contributed to the increase of $[\text{Ca}^{2+}]_i$, because completely treating Sf9 cells with CdCl_2 (5 mM), a Ca^{2+} channels blocker, R-III (100 $\mu\text{g}/\text{mL}$) induced a transient elevation of $[\text{Ca}^{2+}]_i$ in case of cells either in presence of Ca^{2+} containing or Ca^{2+} free solution. In these conditions, pH_i showed similar changes with that of $[\text{Ca}^{2+}]_i$ on the whole. Accordingly, we supposed that there was a certain linkage for change of $[\text{Ca}^{2+}]_i$, cell cycle arrest, proliferation inhibition in Sf9 cells induced by R-III.

Key word: rhodojaponin-III; intracellular free calcium; intracellular pH; Sf9 cells arrest

1. Introduction

Rhodojaponin-III (R-III, Figure 1) show structure as Figure 1 is a grayanoid diterpene isolated from *Rhododendron molle* and determined as the main insecticidal ingredient in the plant [1]. It is an effective natural insecticide against more than 40 species of agricultural pests [2]. Previous studies indicate that R-III shows many anti-insect properties including potent antifeedant, oviposition, oviducts, antimolting, growth inhibitor, contact and/or stomach toxicity [3], which is related to the nervous, digestive, endocrine and reproductive systems of insects. There have been some studies on the mode of action of R-III on insects, although the precise molecular mechanism is not well understood. Some researchers demonstrated that R-III remarkably decreases the contents of acetylcholine (ACh) and has reversible activated effects on $\text{Na}^+\text{-K}^+\text{-ATPase}$ and $\text{Ca}^{2+}\text{-Mg}^{2+}\text{-ATPase}$ activities [4], indicating its interference with insect nervous system through blocked the transition of nervous impulse [5], in which Ca^{2+} as an intracellular second messenger plays a key role.

Figure 1. Structure of Rhodojaponin-III.



Intracellular free calcium ($[\text{Ca}^{2+}]_i$) is a highly versatile intracellular second messenger and signal transducer in both excitable and non-excitable cells. It is involved in many functions in proliferative cells, including gene expression, protein synthesis, cell secretion, motility, metabolism, cell-cycle progression and apoptosis cell death [6,7]. Under normal conditions, $[\text{Ca}^{2+}]_i$ concentration is maintained at 10–100 nM, but sustained Ca^{2+} release from intracellular Ca^{2+} stores, Ca^{2+} influx through receptor- or voltage-dependent Ca^{2+} channels or blockage of re-uptake can perturb $[\text{Ca}^{2+}]_i$ homeostasis [7]. A variety of physical, chemical, or biological stimuli can modify $[\text{Ca}^{2+}]_i$ which may lead to cellular physiological changes such as cell arrest or cell death [8,9].

Intracellular pH (pH_i) is becoming evident to many aspects of cell physiology, and protons may also function as a second messenger in a manner similar to that of Ca^{2+} [10]. Relatively small changes in pH_i could have a profound effect on a variety of cellular functions. For example, changes in pH_i take place in response to growth, tumor promotion, DNA synthesis [11], protein synthesis, activation of the ion channel [12], apoptosis, proliferation and transformation [13]. High pH_i can sensitize cellular proteins such as enzymes, ion channels and ion transporters [14] and pH_i shifts may have significant effects on calcium regulation in cells. It has been established in previous research that pH_i and $[\text{Ca}^{2+}]_i$ are closely linked. In effect, pH_i has been described as being able to affect intracellular Ca^{2+} homeostasis and contribute to the length, magnitude, and frequency of the Ca^{2+} signal through the

modulation of voltage-dependent or -independent plasma membrane Ca^{2+} channels and/or through regulation of the mobilization of Ca^{2+} from internal stores [10]. On the other hand, Ca^{2+} has been described as inducing pH_i variation, particularly in neurons [15]. In several cellular models cytosolic alkalinization is a sufficient signal to release calcium from intracellular pools [16].

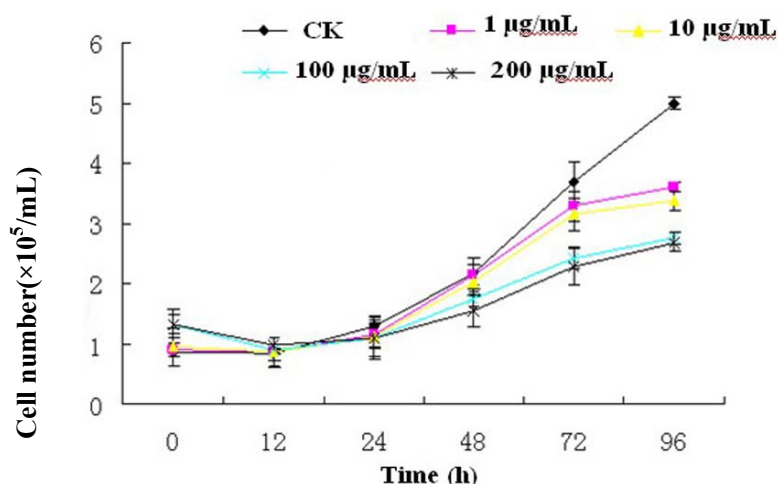
Although many studies on $[\text{Ca}^{2+}]_i$ and pH_i have been carried out due to their importance in regulation of different cellular functions, most of the previous studies are focused on human or mammalian cells and similar studies in insect cells are lacking. Studying the mode of action of botanical pesticide against insects has been greatly simplified by the finding that its effects can be seen in cultured insect cells [17,18]. Therefore, the purpose of this study is to principally characterize the effect of R-III on intracellular Ca^{2+} and pH_i in Sf9 cells (isolated from *Spodoptera frugiperda* pupal ovarian tissue). Otherwise, we primarily discuss the possible interactions among changes of $[\text{Ca}^{2+}]_i$ level, cell cycle and cell proliferation, and the possible linkage between changes of intracellular Ca^{2+} and that of pH_i in Sf9 cells induced by R-III, all of which are helpful to explore some new clues for the further study on insecticidal mechanism of R-III.

2. Results and Discussion

2.1. Effect of R-III on the Proliferation of Sf9 Cells

To investigate the effect of R-III on the proliferation of Sf9 cells, cell viability was measured by Trypan blue exclusion assay. As shown in Figure 2, the inhibition effect of R-III on Sf9 cells was not significant and survival cell after 24 h of treatment with 1, 10, 100 and 200 $\mu\text{g}/\text{mL}$ of R-III was about 1.0×10^5 cells/mL, similar to that of control. After 24 h of treatments with different concentrations of R-III, cell viability decreased in a time- and dose-dependent manner.

Figure 2. Effects of R-III on the proliferation of Sf9 cells. The cells were grown in presence of 1, 10, 100 and 200 $\mu\text{g}/\text{mL}$ of R-III for the times shown in the figure. Survival cell number was counted by means of Trypan blue exclusion with a standard haemocytometer. Each result derived from the mean of three repetitions.

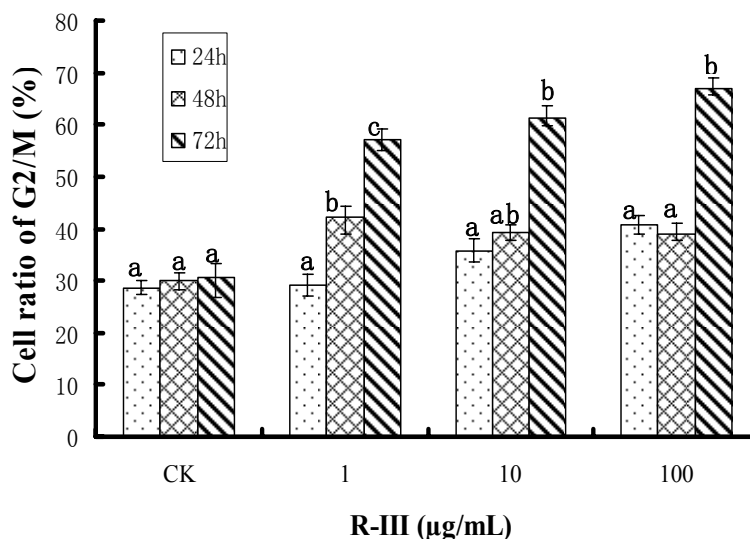


Survival cell number was 3.2×10^5 , 3.0×10^5 , 2.2×10^5 , 2.1×10^5 cells/mL, which was far lower than that of the control (3.8×10^5 cells/mL) after 72 h of treatment with R-III at the concentrations of 1, 10, 100 and 200 $\mu\text{g/mL}$ respectively. By 96 h of treatments with R-III, survival cell number in control (5.0×10^5 cells/mL) had greatly outstripped the R-III treatment. In addition, the inhibition effect on Sf9 cells of R-III at the concentrations of 100 $\mu\text{g/mL}$ and 200 $\mu\text{g/mL}$ was significantly higher than that of 1 $\mu\text{g/mL}$ and 10 $\mu\text{g/mL}$. However, the inhibition effect between 100 $\mu\text{g/mL}$ and 200 $\mu\text{g/mL}$ or between 1 $\mu\text{g/mL}$ and 10 $\mu\text{g/mL}$ showed no significant difference. The results in this assay indicated that R-III strongly inhibited the proliferation of Sf9 cells in a time- and dose-dependent manner.

2.2. Effect of R-III on Cell Cycle

In order to further clarify the effects of R-III on the proliferation of Sf9 cells, we checked the effect of R-III on cell cycle by flow cytometry. As shown in Figure 3, an arrest in G2/M cell cycle phase became evident in Sf9 cells treated with R-III, showing a time- and dose-dependent manner. After 24 h of treatment with 1, 10 and 100 $\mu\text{g/mL}$ of R-III, the percentages of cells in G2/M phase increased to 29.2%, 35.8%, and 40.7% respectively. While after 48 h of the same treatment, the percent of cells in G2/M phase increased to 42.2%, 39.4% and 39.1% and became 57.1%, 61.3% and 67% respectively, after 72 h of treatment. Comparing to the treated groups, the percent of G2/M phase cells in control was lower (28.6%, 29.9% and 30.5% for 24, 48 and 72 h, respectively) and kept in a steady state within the treated time. Results suggested that R-III like the antimitotic agents such as colchicine and azadirachtin [19] interfered with Sf9 cells division and arrests them in G2/M, showing strong inhibitory activity to the cell growth and proliferation.

Figure 3. Effects of R-III on cell cycle. The cells were grown in presence of 1, 10, and 100 $\mu\text{g/mL}$ of R-III for the times shown in the figure. Cell cycle was arrested in G2/M in Sf9 cells and showed a time- and dose-dependent manner. Cells that treated with 0.1% DMSO were used as control. The error bars represent mean \pm SEM for data derived from three repetitions. Treatment means sharing the same letter were not significantly different from each other ($P < 0.05$).



2.3. Effects of R-III on $[Ca^{2+}]_i$ and pH_i in Sf9 Cells

In order to know the effects of R-III on $[Ca^{2+}]_i$, Sf9 cells were exposed to Hanks, a buffer solution containing Ca^{2+} . Ca^{2+} influx took place in Sf9 cells stimulated by R-III, which elicited a significant increase of $[Ca^{2+}]_i$. As shown in Figure 4A1, comparing to control, Sf9 cells showed gradual increase of $[Ca^{2+}]_i$ by 29.9%, 38.28%, 64.21% and 111.78%, after the stimulation with 1, 10, 100 and 200 $\mu\text{g/mL}$ of R-III respectively, showing a dose-dependent fashion. Under these conditions, we observed a similar change of pH_i with that of $[Ca^{2+}]_i$. As shown in Figure 4B1, Sf9 cells presented a gradual increase of pH_i by 22.27%, 37.13%, 69.17% and 89.58% after stimulation with 1, 10, 100 and 200 $\mu\text{g/mL}$ of R-III respectively, also in a dose-dependent fashion. The increase of pH_i was only 5.7% in control. In order to further investigate the effects of R-III on $[Ca^{2+}]_i$ in Sf9 cells, we checked the time-dependent changes of Ca^{2+} fluorescence signals in Sf9 cells induced by R-III. As shown in Figure 4A-a, a flat trace in control indicated no change of $[Ca^{2+}]_i$ in cells. A transient elevation of $[Ca^{2+}]_i$ characterized by a fluorescence intensity increase followed by a recovery to basal level was observed in Sf9 cells stimulated with low concentration of R-III (1 $\mu\text{g/mL}$) (Figure 4A-b), suggesting that cells can regulate $[Ca^{2+}]_i$ to keep intracellular Ca^{2+} homeostasis in case of slight external stimulation.

Figure 4. Effect of R-III on $[Ca^{2+}]_i$ and pH_i in Sf9 cells in presence of Hanks. **(A1)**. changes of $[Ca^{2+}]_i$ in Sf9 cells stimulated by R-III at various concentrations as indicated by relative change of Fluo-3AM fluorescence intensity; **(B1)**. Changes of pH_i in Sf9 cells stimulated by R-III at various concentrations as indicated by relative change of Snarf1M fluorescence intensity; **(A a–d)**. Dynamic changes of $[Ca^{2+}]_i$ indicated by a dynamic trace of Fluo-3AM fluorescence intensity in case of Sf9 cells treated with 0, 1, 100, 200 $\mu\text{g/mL}$ of R-III respectively; **(B a–d)**. pH_i profile in cells subject to the protocol in **(A a–d)**; **(A-e)**. Dynamic variation of $[Ca^{2+}]_i$ in Sf9 cells treated with 100 $\mu\text{g/mL}$ of R-III for two times; **(B-e)**. pH_i profile in cells subject to the protocol in **(A-e)**. Arrows indicated the addition of R-III. Results of representative experiment derived from three repetitions and 4–6 cells were measured in each repetition. The error bars represent mean \pm SEM for data derived from value of relative fluorescence intensity in each time interval. Treatment means sharing the same letter were not significantly different from each other ($P < 0.05$).

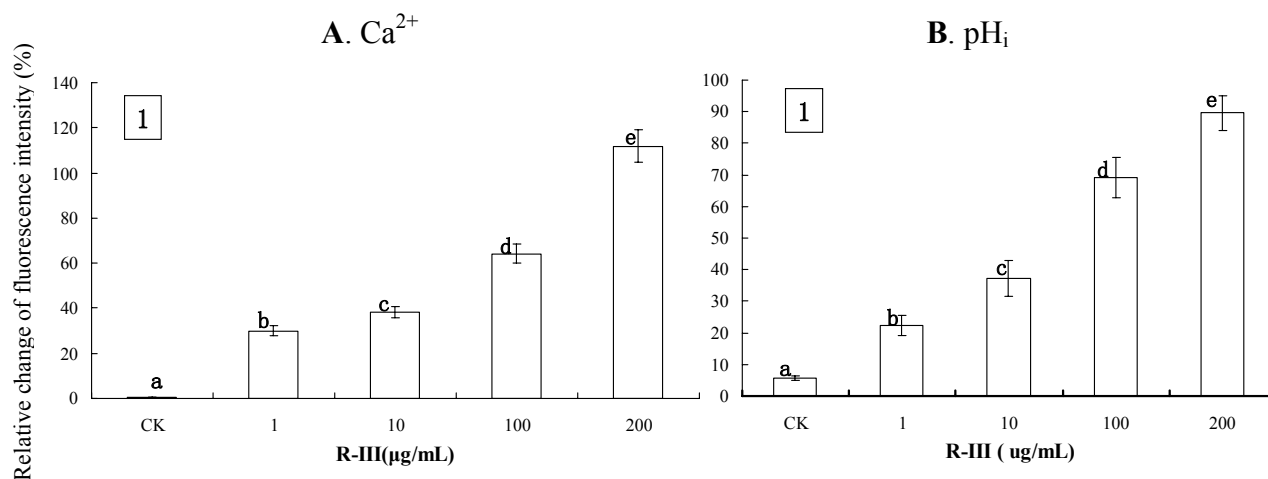


Figure 4. Cont.

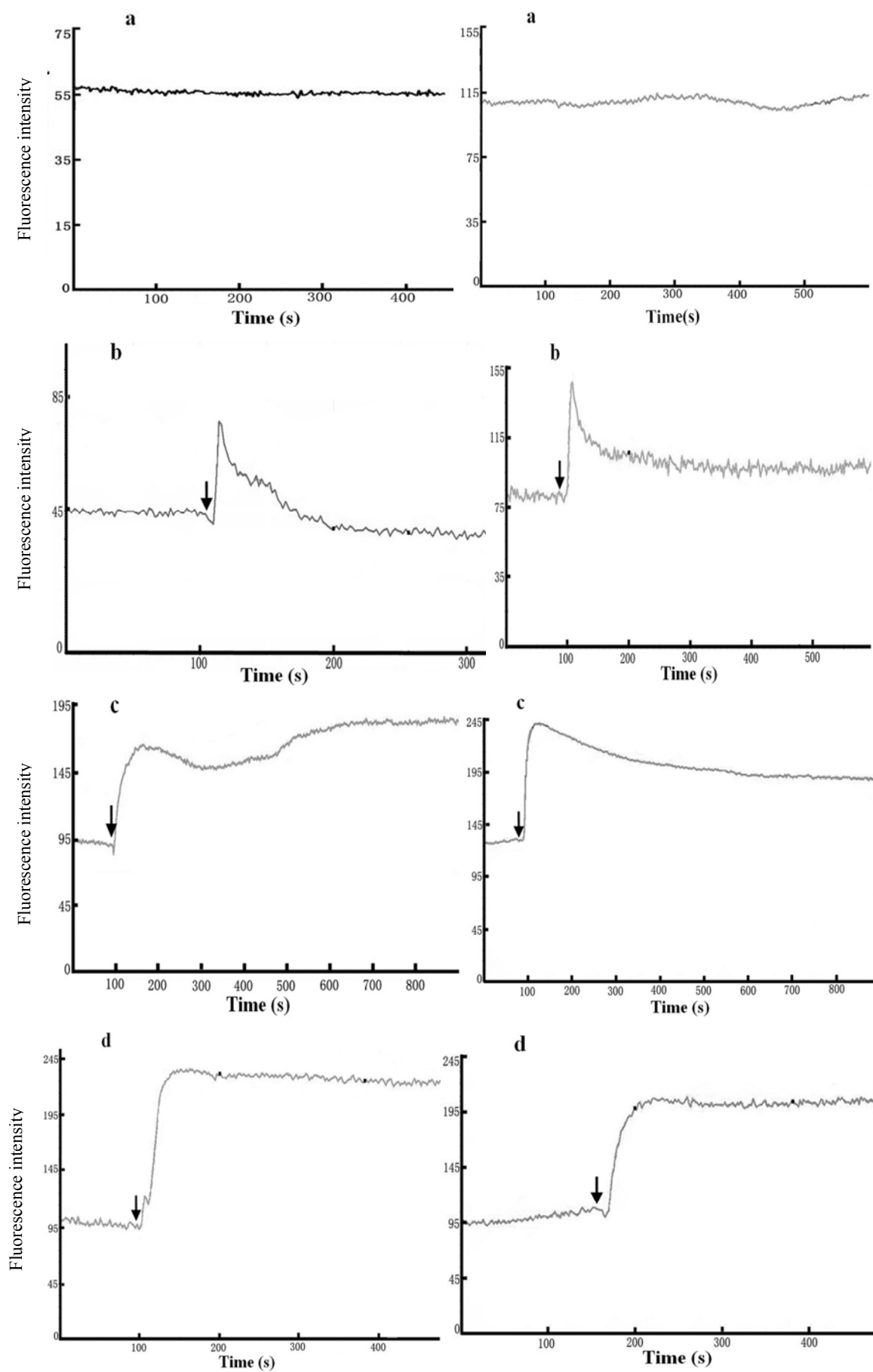
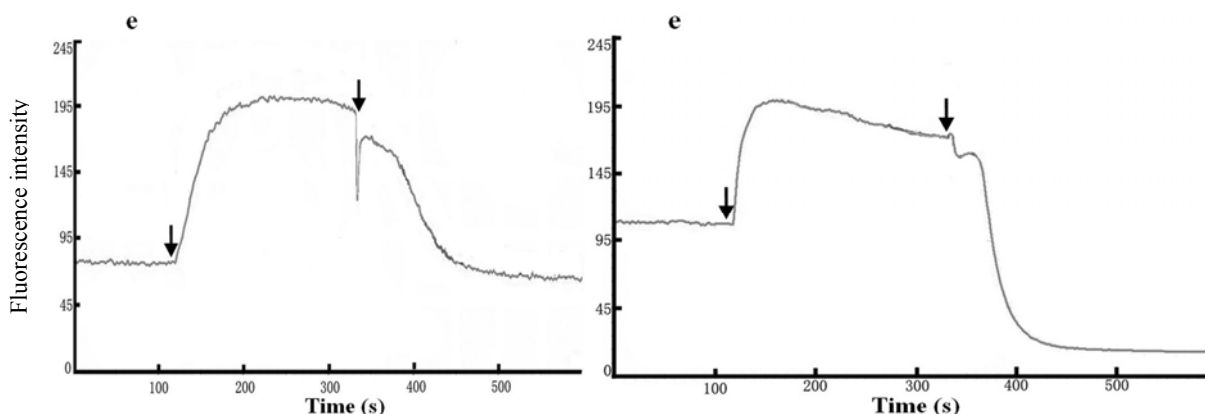


Figure 4. Cont.



When exposed to 100 and 200 $\mu\text{g/mL}$ of R-III, Sf9 cells showed a rapid rise of $[\text{Ca}^{2+}]_i$, which reached to a high steady state [Figures 4A-(c,d)]. Previous studies have established that elevation of $[\text{Ca}^{2+}]_i$ may derive from extra cellular Ca^{2+} influx through calcium channels or transporters [20] or the Ca^{2+} release from intracellular Ca^{2+} stores induced by intracellular inositol 1,4,5-trisphosphate (IP3), synthesized in response to external stimulation [21]. Under this condition, we applied the second stimulation of R-III, which caused $[\text{Ca}^{2+}]_i$ declining sharply in a index fashion to a steady state lower than the basal level (Figure 4A-e). In this assay, we also found that the changes of pH_i were in line with that of $[\text{Ca}^{2+}]_i$, as shown in the traces in Figures 4B-(a,d) and the second stimulation of R-III also produced a sharply decrease of pH_i to a steady state lower than the basal level (Figure 4B-e). Although the mechanisms of the sharp decrease of $[\text{Ca}^{2+}]_i$ and pH_i are not clear yet, an interpretation from groups of Li *et al.* [22] who investigated the modulation effect of glutamate on $[\text{Ca}^{2+}]_i$ of inner hair cell of the guinea pig cochlea and found similar phenomenon may enlighten us on this study: Excessive stimulation of glutamate may cause toxicity on cells and increase the penetration of plasma membrane (PM) which gives rise to $[\text{Ca}^{2+}]_i$ efflux. Since R-III was a botanic pesticide showing significant toxicity to many kinds of insect, the second stimulation of R-III possibly produced toxic effect on Sf9 cells causing $[\text{Ca}^{2+}]_i$ efflux, in agreement with viewpoint of [22], and $[\text{Ca}^{2+}]_i$ efflux exchanged for H^+ influx through Ca^{2+} -ATPase in PM [23], eliciting decrease of pH_i .

2.4. Effects of R-III on $[\text{Ca}^{2+}]_i$ and pH_i in Sf9 Cells in Presence of Dhanks

To further clarify the effect of R-III on $[\text{Ca}^{2+}]_i$ and pH_i , Sf9 cells were exposed to Dhanks, a Ca^{2+} -free buffer solution, and recoded the change of fluorescence intensity in Sf9 cells stimulated with R-III (100 $\mu\text{g/mL}$) at 130 s. Comparing to the control with only a slightly decrease of $[\text{Ca}^{2+}]_i$ (3.52%) (Figure 5A1, A-a), $[\text{Ca}^{2+}]_i$ sharply decreased by 24.64% after the stimulation of R-III (Figure 5A1), and kept in a steady state (Figure 5A-b), indicating $[\text{Ca}^{2+}]_i$ efflux in Sf9 cells induced by R-III, and no increase of $[\text{Ca}^{2+}]_i$ was observed in case of re-addition of CaCl_2 (2 μM) to the Ca^{2+} -free buffer solution at 500 s (Figure 5A-b), suggesting that Ca^{2+} efflux in cells was irreversible. Previous study finds that although glucose oxidase induce a rapid decrease in rat endothelial cells exposed in Ca^{2+} free buffer, re-addition of Ca^{2+} to the extracellular buffer may activate store operated Ca^{2+} entry to cause large $[\text{Ca}^{2+}]_i$ increases [24]. However, store operated Ca^{2+} entry in Sf9 cells was not activated by the

re-addition of Ca^{2+} in this assay. The results further proved that it was the Ca^{2+} influx that elicited the substantial increase of $[\text{Ca}^{2+}]_i$ in Sf9 cells stimulated by R-III in case of cell exposure to Hanks in the experiment above [Figures 4A-(b,e)]. Under these conditions, pH_i also showed significant decrease (17.85%), and sustained decrease (61.02%) was observed even if addition of CaCl_2 at 130 s after stimulation (Figure 5B1). Knowing from dynamic change of fluorescence signals in Sf9 cells induced by R-III (Figure 5B-b), R-III induced a transient rise of pH_i , followed by a decline to a steady level much lower than basal level in Sf9 cells, and no recovery of pH_i was observed even if addition of CaCl_2 at 130 s after stimulation. In contrast, the control showed only a slightly decrease of pH_i (Figure 5B-a). Interestingly, $[\text{Ca}^{2+}]_i$ showed no transient increase in the same conditions (Figure 5A-b). The results in this assay indicated that R-III not only induced $[\text{Ca}^{2+}]_i$ in Sf9 cells decline through Ca^{2+} efflux but also elicited the intracellular acidification, possibly through H^+ entry in exchange for Ca^{2+} extrusion by the Ca^{2+} -ATPase in cell PM [23].

Figure 5. Effects of R-III on $[\text{Ca}^{2+}]_i$ and pH_i in Sf9 cells in presence of Dhanks. **(A1)**. Changes of $[\text{Ca}^{2+}]_i$ when cells were stimulated by 100 $\mu\text{g}/\text{mL}$ in 130 s and subsequent addition of 2 μM CaCl_2 in 500 s, as indicated by relative change of Fluo-3AM fluorescence intensity; **(A-a)**. Control; **(A-b)**. Dynamic changes of $[\text{Ca}^{2+}]_i$ in the same conditions with **(A1)**; **(B)**. pH_i profile in cells subjected to the protocol in **(A)**. Results of representative experiment derived from three repetitions and 4–6 cells were measured in each repetition. The error bars represent mean \pm SEM for data derived from value of relative fluorescence intensity (vs. control) in each time interval. Treatment means sharing the same letter were not significantly different from each other ($P < 0.05$). The negative value meant decrease of relative fluorescence intensity in cells.

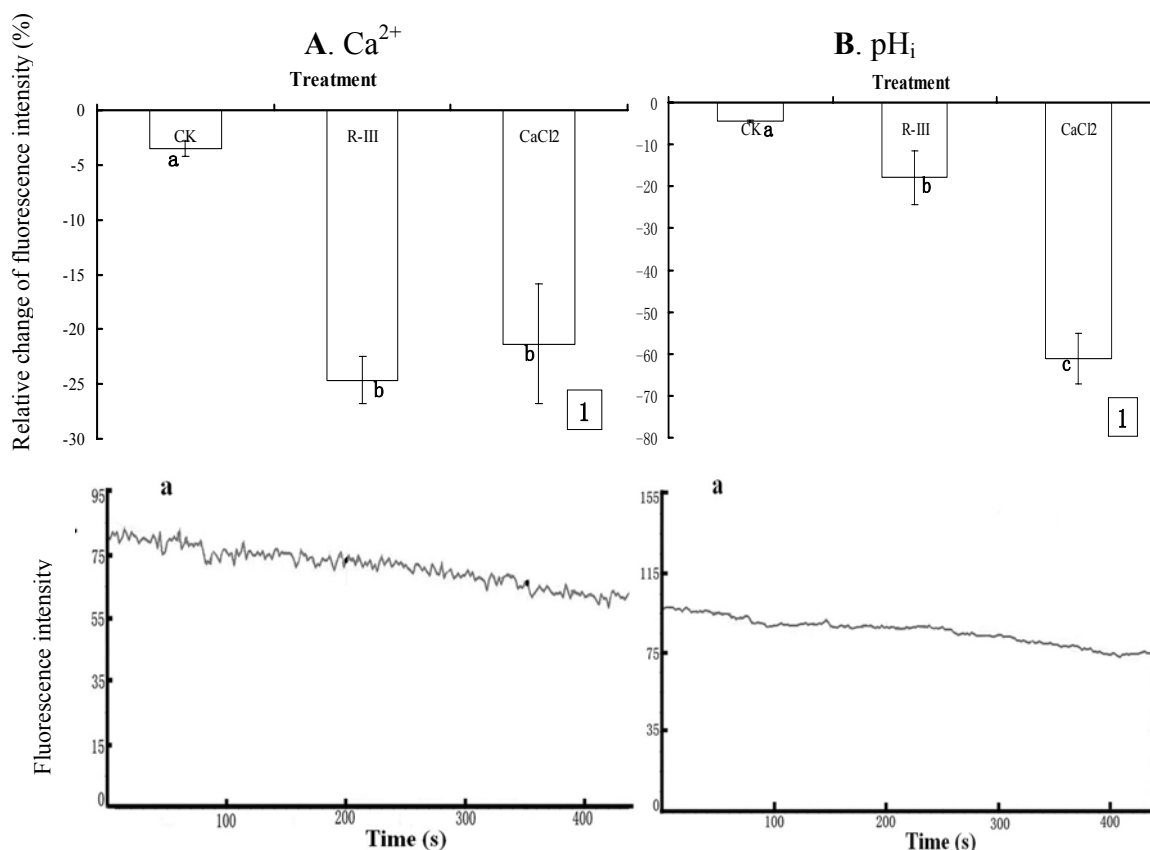
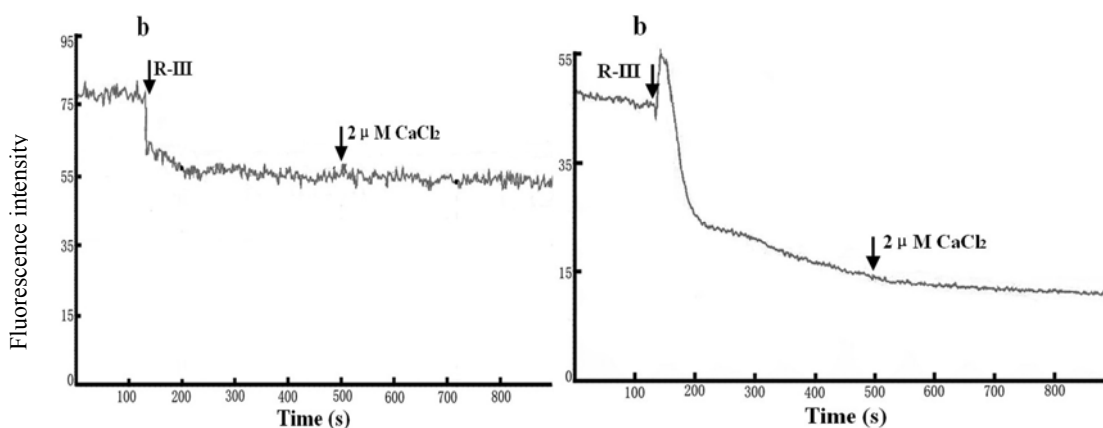


Figure 5. Cont.



Ca^{2+} signaling plays a crucial role in the function of almost all cell types as an intracellular second messenger [25]. For example, many researches prove that changes in $[\text{Ca}^{2+}]_i$ homeostasis are associated with induction of apoptotic [26] or cell death [27]. An experimental report coming from group of Wang *et al.* [28] provides a convincing interpretation for the role of Ca^{2+} in participation in apoptotic cell death. In their study, the authors found that H_2O_2 -induced apoptosis of tobacco protoplasts primarily involves in the increase of $[\text{Ca}^{2+}]_i$ resulting from the entry of extra cellular Ca^{2+} . In recent years, some reports show that calcium signal is a key component of the molecular switch mechanism in cell division cycle [29]. Through the interplay with several proteins, $[\text{Ca}^{2+}]_i$ participates in regulating key steps in the cell cycle such as reentry of quiescent cells into proliferation and the transition through the G1/S, G2/M, and the metaphase/anaphase boundaries [30-32]. Moreover, mitosis can be initiated by IP_3R -induced calcium transients [33]. Disturbance of $[\text{Ca}^{2+}]_i$ homeostasis such as increase of $[\text{Ca}^{2+}]_i$ level in response to external stimulation may interfere with cells division cycle, resulting in cell cycle arrest [34]. In present study, Sf9 cells showed significant changes of $[\text{Ca}^{2+}]_i$ induced by R-III [Figures 4A-(b,e) and Figure 5A-b]. Otherwise, R-III also produced cell cycle arrest in G2/M (Figure 3) and strongly inhibited Sf9 cells proliferation (Figure 2), although apoptosis was not observed. Our results suggested that there was a certain linkage for change of $[\text{Ca}^{2+}]_i$, cell cycle arrest, cell proliferation inhibition in Sf9 cells induced by R-III. Moreover, we tentatively hypothesize that disturbance of $[\text{Ca}^{2+}]_i$ homeostasis in Sf9 cells induced by R-III may result in cell cycle arrest, which finally causes inhibition of insect cells proliferation or even cell death (including apoptotic cell death). This dual negative effect would significantly decrease the absolute number of cells, and finally induce remarkable decrease of survival cell number in R-III treatment.

2.5. The Contribution of Intracellular Ca^{2+} Stores to the Changes of Intracellular Ca^{2+} and pH_i

Intracellular Ca^{2+} stores such as mitochondria or endoplasmic reticulum may be the other principal source of Ca^{2+} [35]. In present study, to examine the contribution of intracellular Ca^{2+} stores to the changes of intracellular Ca^{2+} , CdCl_2 , a blocker of Ca^{2+} channels was used to treat the cells that were then exposed to Hanks in the following experiments. CdCl_2 (5 mM) was applied to treat the cells for 200 s prior to the stimulation of R-III (100 $\mu\text{g}/\text{mL}$). As shown in Figure 6A1 and Figure 6B1, $[\text{Ca}^{2+}]_i$ and pH_i in Sf9 cells incubated with CdCl_2 showed a slight decrease (4.52% and 3.03% respectively).

After treatment with R-III, $[Ca^{2+}]_i$ and pH_i rose by 235% and 40.32% respectively. As indicated in dynamic change of trace (Figures 6A-a and B-a), $[Ca^{2+}]_i$ increased immediately, but followed by a gradual decrease when cells were stimulated by R-III, suggesting that Cd^{2+} gradually blocked the Ca^{2+} channels to inhibit the Ca^{2+} influx.

Figure 6. Effect of Ca^{2+} channels block on $[Ca^{2+}]_i$ and pH_i in R-III-induced Sf9 cells in presence of Hanks. (A1). changes of $[Ca^{2+}]_i$ in Sf9 cells treated with 0.5 mM $CdCl_2$ for 200 s and 10 min prior to stimulate with R-III (100 $\mu g/mL$), as indicated by relative change of Fluo-3AM fluorescence intensity; (A-a). Dynamic changes of $[Ca^{2+}]_i$ in Sf9 cells treated with 0.5 mM $CdCl_2$ for 200 s prior to stimulate with R-III (100 $\mu g/mL$); (A-b). Dynamic changes of $[Ca^{2+}]_i$ in Sf9 cells incubated with $CdCl_2$ (5 mM) for 10 min prior to stimulated with R-III (100 $\mu g/mL$); (B). pH_i profile in cells subjected to the protocol in (A). Results of representative experiment derived from three repetitions and 4–6 cells were measured in each repetition. The error bars represent mean \pm SEM for data derived from value of relative fluorescence intensity in each time interval. Treatment means sharing the same letter were not significantly different from each other ($P < 0.05$). The negative value meant decrease of relative fluorescence intensity in cells.

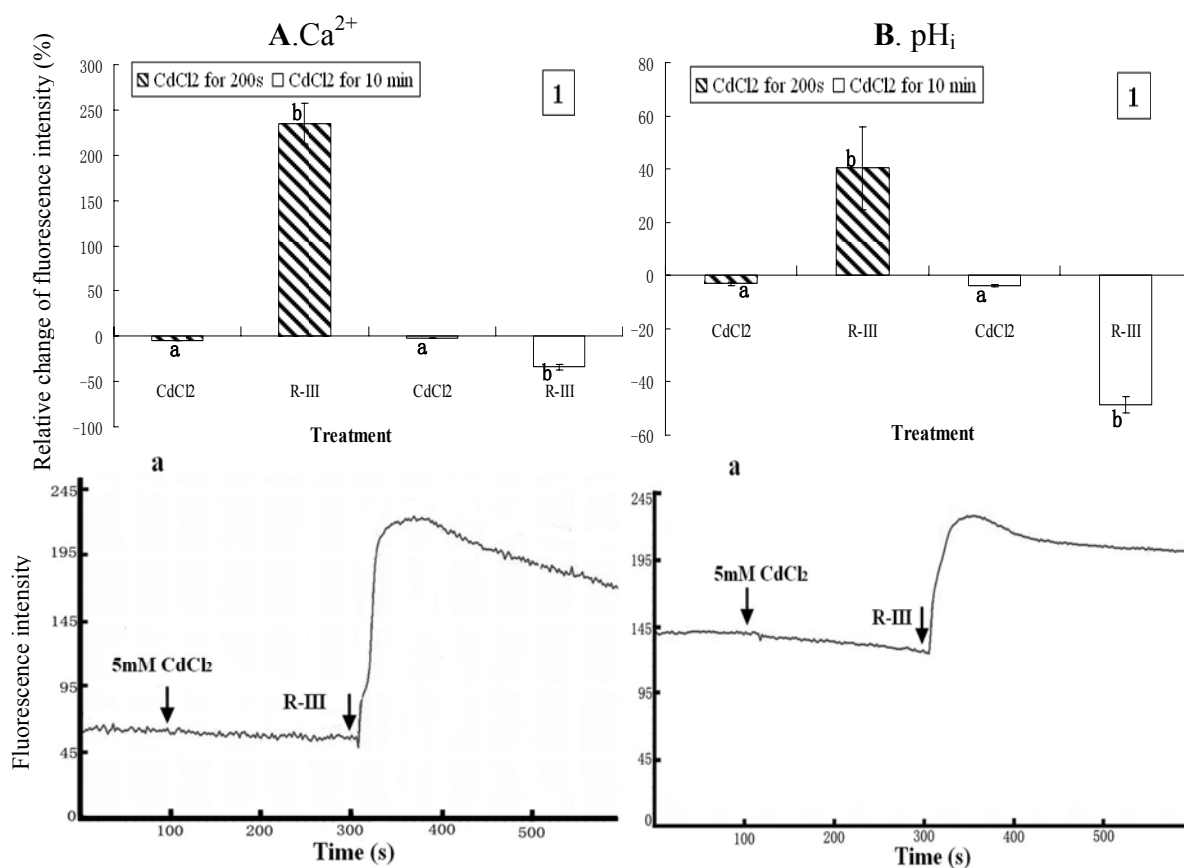
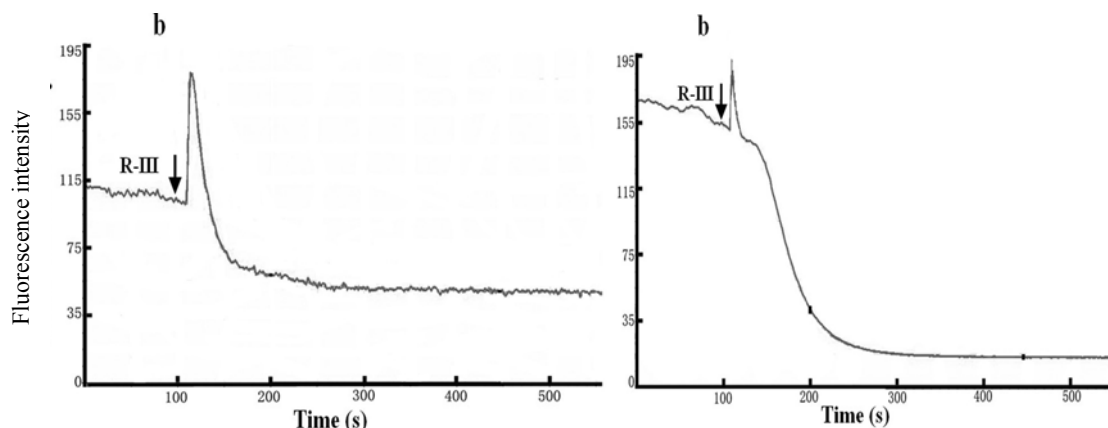


Figure 6. Cont.



Under these conditions, pH_i changed in similar fashion with $[\text{Ca}^{2+}]_i$. When we used CdCl_2 (5 mM) to incubate with Sf9 cells for 10 min to block the Ca^{2+} channels completely, and then stimulated with R-III (100 g/mL), both $[\text{Ca}^{2+}]_i$ and pH_i decreased sharply by rate of 33.85% and 48.74% respectively (Figures 6A1 and 6B1). However, in this condition, we found in dynamic change of trace of Figure 6A-b and Figure 6B-b that both $[\text{Ca}^{2+}]_i$ and pH_i showed a transient elevation before decreasing sharply. Since Cd^{2+} had blocked Ca^{2+} channels completely and inhibited Ca^{2+} influx, the transient increase of $[\text{Ca}^{2+}]_i$ mainly derived from Ca^{2+} released from intracellular Ca^{2+} stores. It is well established that inositol 1,4,5-trisphosphate (IP_3), synthesized in response to external stimulation, induces the release of Ca^{2+} from intracellular stores [21]. In this assay, stimulation of R-III may also induce the synthesis and increase of IP_3 to promote release of Ca^{2+} from intracellular stores through the Ca^{2+} -ATPase. Otherwise, the Ca^{2+} sustained release from intracellular Ca^{2+} stores may likely give rise to its depletion, which could activate store-operated Ca^{2+} channels to promote the Ca^{2+} influx in mammalian non-excitable cells [36], whereas Ca^{2+} channels had been blocked completely by CdCl_2 , and no Ca^{2+} entry but efflux characterized by sharp decline of $[\text{Ca}^{2+}]_i$ to a level far lower than basal level occurred in this study (Figure 6A-b). Under this condition, we observed a proportional change of pH_i with that of $[\text{Ca}^{2+}]_i$. We hypothesized that Ca^{2+} released from intracellular stores through the Ca^{2+} -ATPase in exchange for H^+ entry intracellular stores resulted in the transient increase of pH_i , and the Ca^{2+} -ATPase of PM was activated by the transient increase of $[\text{Ca}^{2+}]_i$ and the sustained stimulation of R-III. $[\text{Ca}^{2+}]_i$ effused through Ca^{2+} -ATPase in exchange for H^+ entry intracellular cytosol, which caused the decrease of pH_i . The results in this assay demonstrated that both extra calcium influx and Ca^{2+} release from intracellular Ca^{2+} stores contributed to the elevation of $[\text{Ca}^{2+}]_i$ in Sf9 cells stimulated by R-III, and pH_i showed proportional change with $[\text{Ca}^{2+}]_i$ in response to the stimulation of R-III.

To further clarify the sources of Ca^{2+} and the response of intracellular Ca^{2+} stores in Sf9 cells stimulated by R-III, we repeated the above experiment with the only different condition of cells being exposed to Dhanks. As shown in Figure 7A and Figure 7B, $[\text{Ca}^{2+}]_i$ and pH_i of Sf9 cells indicated only a slight decline in case of incubation with CdCl_2 for 200s or 10 min. However, the subsequent addition of stimulation by R-III to Sf9 cells after incubation with CdCl_2 for 200 s gave rise to a dramatic decrease of pH_i by rate of 73.36% and only a slight decrease of $[\text{Ca}^{2+}]_i$ (11.55%) (Figure 7A1 and Figure 7B1). Under this condition, we got the information from Figure 7A-a that $[\text{Ca}^{2+}]_i$ showed only a transient increase followed by a rapid recovery to the basal level, which explained well the only slight

change of $[Ca^{2+}]_i$ in this time interval. Since cells were in presence of Ca^{2+} free solution, and Ca^{2+} channels in PM were at least partially blocked, the transient increase of $[Ca^{2+}]_i$ should mainly derive from intracellular Ca^{2+} stores, which further prove the contribution of intracellular Ca^{2+} stores to the changes of intracellular Ca^{2+} .

Figure 7. Effect of Ca^{2+} channels block on $[Ca^{2+}]_i$ and pH_i in R-III-induced Sf9 cells in presence of Dhanks. **(A1)**. changes of $[Ca^{2+}]_i$ in Sf9 cells treated with 0.5 mM $CdCl_2$ for 200 s and 10 min prior to stimulate with R-III (100 μ g/mL), as indicated by relative change of Fluo-3AM fluorescence intensity; **(Aa)**. Dynamic changes of $[Ca^{2+}]_i$ in Sf9 cells incubated with $CdCl_2$ (5 mM) for 200 s prior to stimulate with R-III (100 μ g/mL); **(A-b)**. Dynamic changes of $[Ca^{2+}]_i$ in Sf9 cells incubated with $CdCl_2$ (5 mM) for 10 min prior to stimulate with R-III (100 μ g/mL) for two times; **(B)**. pH_i profile in cells subjected to the protocol in **(A)**. Results of representative experiment derived from three repetitions and 4–6 cells were measured in each repetition. The error bars represent mean \pm SEM for data derived from value of relative fluorescence intensity in each time interval. Treatment means sharing the same letter were not significantly different from each other ($P < 0.05$). The negative value meant decrease of relative fluorescence intensity in cells.

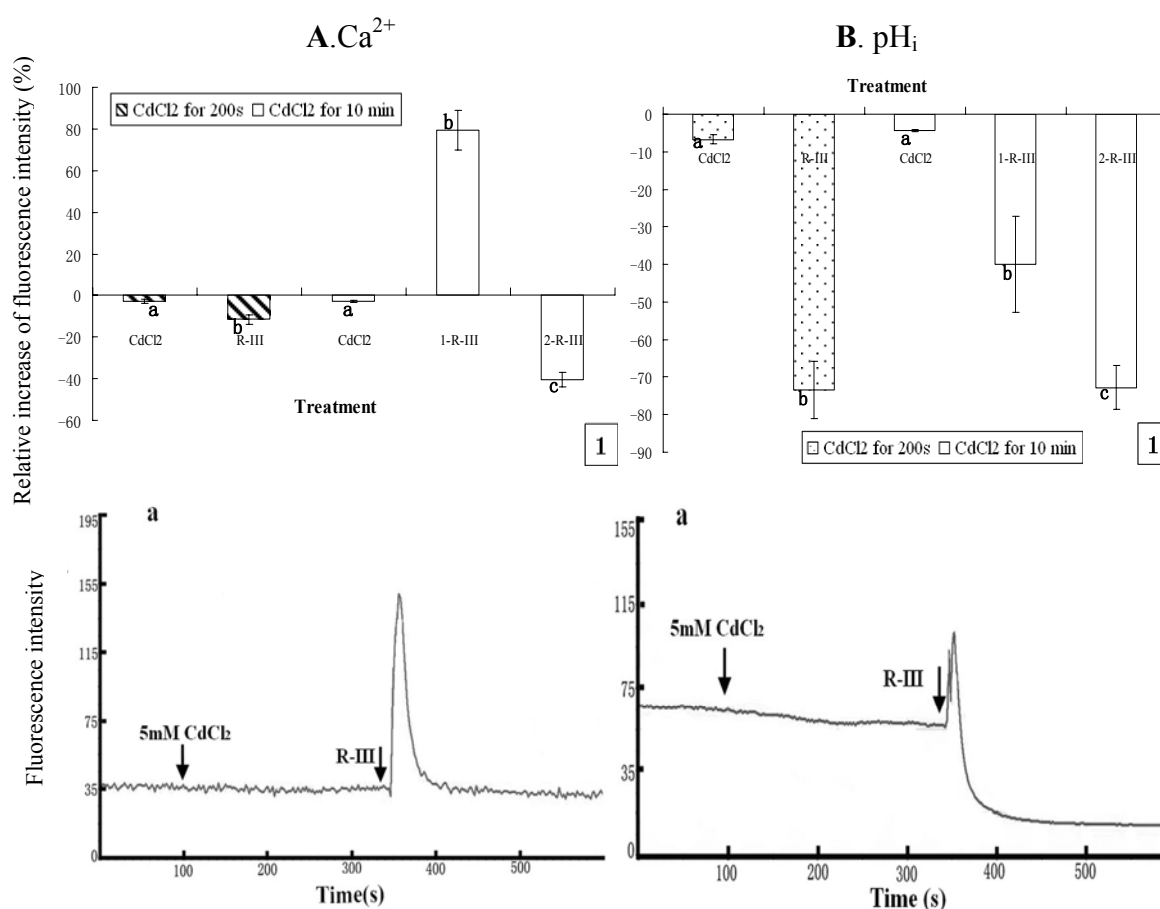
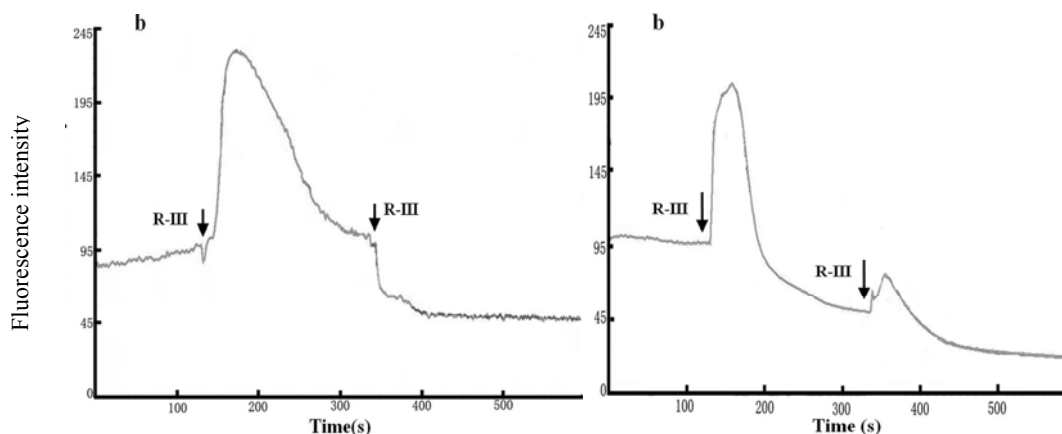


Figure 7. Cont.



Meanwhile, pH_i under these conditions also showed a transient increase similar with that of $[\text{Ca}^{2+}]_i$, but decline finally to a state much lower than the basal level (Figure 7B-a), which induced a high rate of pH_i decrease (Figure 7A1) differing from the change of $[\text{Ca}^{2+}]_i$. Nevertheless, cells pretreated for 10 min with CdCl_2 (5 mM) presented a markedly increase of $[\text{Ca}^{2+}]_i$ by rate of 79.43% in the first stimulation of R-III for 200 s, and the second stimulation of R-III induced $[\text{Ca}^{2+}]_i$ decrease by 40.35% (Figure 7A1). Knowing from the dynamic trace in Figure 7A-b, $[\text{Ca}^{2+}]_i$ in Sf9 cells showed a transient elevation followed by a gradual decline to basal level in the first stimulation of R-III, which made the peak of dynamic trace much wider than that of Figure 6A-b, suggesting that $[\text{Ca}^{2+}]_i$ was much higher in this time interval. In contrast, R-III induced a decrease of pH_i by rate of 39.85% in first stimulation and 72.78% in the second stimulation (Figure 7B1). We found from Figure 7B-b that pH_i in Sf9 cell also showed a transient elevation, but followed by a rapid decline in the first stimulation of R-III. The peak of dynamic trace also became wider comparing to that of Figure 6A-b. Although the reason for these phenomenon was not clear, the results in this assay further indicated that pH_i showed proportional change with $[\text{Ca}^{2+}]_i$ in response to the stimulation of R-III on the whole.

It is known that the functional relationships and crosstalk between calcium and pH receive more and more attention, specially, on human cells, but little on insect cells. Although many studies show that changes of pH_i are associated with that of $[\text{Ca}^{2+}]_i$ in a number of cell types, a clear relationships between the steady state level of pH_i and $[\text{Ca}^{2+}]_i$ is not observed in present because interrelationships between pH_i and $[\text{Ca}^{2+}]_i$ are rather complex and depend on the cell type [37]. A few studies show that cytosolic alkalization shift is associated with the increase of $[\text{Ca}^{2+}]_i$ [38] and that acidification shift is associated with the decrease of $[\text{Ca}^{2+}]_i$ [39]. More specifically, an experimental report on crayfish muscle fibre from Kaila and Voipio [40] shows that resting cytosolic calcium is decreased by intracellular alkalosis. In present study, the changes of pH_i in Sf9 cells induced by R-III show distinct proportion with that of $[\text{Ca}^{2+}]_i$, which also suggests that cytosolic alkalization or acidification are associated with changes of $[\text{Ca}^{2+}]_i$, but the specific interaction mechanism of pH_i and $[\text{Ca}^{2+}]_i$ in these conditions remains unclear, and need further researches to clarify.

3. Experimental

3.1. Reagents

The Rhodojaponin-III (98%) was isolated by using HPLC from the flowers of *R. molle* in the Laboratory of Insect Toxicology, South China Agricultural University. Fura-3/AM, Snarf1/AM were purchased from Sigma and stock solutions of all molecules were initially dissolved in dimethyl sulfoxide (DMSO), diluted to their final concentration in phosphate buffer solution (135 mM NaCl, 2.7 mM KCl, 1.5 mM KH₂PO₄, and 8 mM K₂HPO₄, pH 7.2) and stored at −20 °C until used. All other chemicals were from standard commercial sources and reagent grade or the highest purity.

3.2. Cell Culture

Sf9 cells were obtained from State Key Laboratory of Biocontrol, Sun Yat-sen University, and were cultured in Grace's medium (GIBCO-BRL, Grand Island, NY, USA) supplemented with 10% fetal bovine serum (heat-inactivated) and 1% penicillin/streptomycin. Cells were cultured at 27 °C and subcultured every 3 days. Confluent cells with >95% viability (tested with Trypan blue exclusion) were used in all experiments.

3.3. Cell Growth Curve

Sf9 cells were seeded onto 24-well plates (2×10^4 cells per well). When cells were adherent, at concentrations of 1, 10, 100 and 200 µg/mL was added to treated cells for serial times (0, 12, 24, 48, 72 and 96 h). Cells that cultured with 0.1% DMSO at the same times were used as control. After harvested, survival cell number for each time point was counted using Trypan blue exclusion test with a standard haemocytometer. Growth curve was made after analyzing the data.

3.4. Flow Cytometry

Sf9 cells were seeded onto a 25 cm² plastic tissue culture flask (2×10^5 cells per flask). When the density was 1×10^6 cells/mL, cells were treated with R-III at concentrations of 1, 10, 100 and 200 µg/mL for serial times (24, 48 and 72 h). After harvested, cells were re-suspended and washed twice with phosphate buffer solution (PBS) (137 mM NaCl, 2.7 mM KCl, 100 mM Na₂HPO₄, 2 mM KH₂PO₄, pH 7.2). After that, cells were fixed in cold 70% ethanol, and stored below −20 °C over night. Prior to analysis, ethanol was removed and fixed cells were washed twice with PBS (pH 7.2). Cells were re-suspended in PI solution (50 µg/mL PI, 0.1% Triton X-100, 0.1 mM EDTA, 50 µg/mL RNase A) and incubated for 30 min at room temperature. After that cells were processed in a FACSCalibur (Becton Dickinson, USA). At least 2.0×10^4 cells were counted in each assay. The fraction of the total cell population presented in G2/M phase was obtained from DNA histograms using Cell Quest and Modfit Software (Becton Dickinson, USA). All cytometry experiments were performed on cells in log phase of growth. Cells that cultured with 0.1% DMSO at the same times were used as control.

3.5. Fluorescence Measurements

Cell treatment: $[Ca^{2+}]_i$ measurements from Sf9 cells were performed with the fluorescent Ca^{2+} indicator fluo-3/AM. Cells were cultured in 35-mm polystyrene tissue culture dishes (Nunc, Denmark) and washed twice with PBS, then loaded with 1 μ M membrane-permeant acetoxymethyl ester of the dye (fluo-3/AM) for 45 min at 37 °C. After dye loading, cells were washed twice with Dhanks solution (137.93 mM NaCl, 5.33 mM KCl, 4.17 mM $NaHCO_3$, 0.441 mM KH_2PO_4 , 0.338 mM Na_2HPO_4 , 5.56 mM D-Glucose, pH 7.2). The pre-treatment measurement of pH_i was carried out same as $[Ca^{2+}]_i$ measurements, except that the final concentration of dye solution were 10 μ M (Snarf1/AM).

Fluorescence measurement: Fluo-3/AM and Snarf1/AM is one of the most suitable Ca^{2+} and pH_i indicators for CLSM, and widely used to monitor $[Ca^{2+}]_i$ and pH_i in various cells. It can be excited by an argon ion laser at 488 nm, and its emitted fluorescence (at wavelengths 520 nm) increases with increasing $[Ca^{2+}]_i$ [41] or pH_i . To measure the Fluo-3/AM and Snarf1/AM fluorescence, laser scanning confocal microscopy (Leica TCS SP2AOBS, Germany) was used to scan the cells with good silhouette and recorded fluorescence at intervals of 6 s for more than 400 s, and room temperature was kept in 20–23 °C during the experiments. According to the experimental design, drug was added from concentrated solutions with a pipette directly into the culture dishes through a small hole on top of the cuvette lid, and in control assays the same volume of DMSO was added. Results were analyzed using the Leica confocal software, and got time-dependent curves of calcium fluorescence signal. Although fluorescence recordings could not be calibrated to count the absolute value of $[Ca^{2+}]_i$ [22], $[Ca^{2+}]_i$ change could be shown by relative change of fluorescence intensity.

3.6. Statistical Analysis

Data analysis was carried out using SAS software (SAS Institute Inc.) and Microsoft Excel software. Differences between the treatments were determined by Tukey's multiple range tests ($P < 0.05$ being considered significant).

4. Conclusions

R-III displayed strong inhibitory activity on the proliferation of Sf9 cells, and interfered with the Sf9 cell division cycle and arrested them in G2/M. In addition, R-III perturbed $[Ca^{2+}]_i$ homeostasis by inducing $[Ca^{2+}]_i$ influx or efflux in Sf9 cells in the presence of Ca^{2+} -containing or Ca^{2+} -free buffer solution. In these conditions, pH_i showed proportional changes with that of $[Ca^{2+}]_i$ on the whole. According to the results and discussion in this paper, we supposed that there was a certain linkage for change of intracellular calcium, cell cycle arrest, cell proliferation inhibition in Sf9 cells induced R-III and that cytosolic alkalization or acidification shifts are associated with changes of $[Ca^{2+}]_i$ level in Sf9 cells induced R-III.

Acknowledgements

We would like to thank National Nature Science Foundation (Number 31071713) and Research Fund for the Doctoral Program of Higher Education of China (20094404110019) for providing funds, Xiang Jing Qin (School of Life Sciences, Sun Yat-sen University, China) for her kind assistance in writing.

References

1. Klocke, J.A.; Hu, M.Y.; Chiu, S.F.; Kubo, I. Grayanoid diterpenes insect antifeedants and insecticides from *Rhododendron molle*. *Phytochemistry* **1991**, *30*, 1797-1800.
2. Hu, M.Y.; Zhong, G.H.; Wu, Q.S.; Chiu, S.F. The biological activities of yellow azalea, *Rhododendron molle* G. Don against the vegetable leafminer, *Liriomyza sativae* (Diptera: Agromyzidae). *Entomologia Sinica* **2000**, *7*, 65-70.
3. Zhong, G.H.; Hu, M.Y.; Wei, X.Y.; Weng, Q.F.; Xie, J.J.; Liu, J.X.; Wang, W.X. Grayanane diterpenoids from the flowers of *Rhododendron molle* with cytotoxic activity against a *Spodoptera frugiperda* cell line. *J. Nat. Prod.* **2005**, *68*, 924-926.
4. Zhong, G.H.; Hu, M.Y.; Chiu, S.F.; Cheng, D.M. Effects of Rhodojaponin-III on nervous System of larvae of imported cabbage worm, *Pieris rapae* L. *Chin. J. Pestic. Sci.* **2000**, *2*, 13-18.
5. Feng, X.; Chiu, S.F. Preliminary studies on the biological activity of extracts from *Rhododendron molle* against insect pests and their mode of action. *J. South China Agric. Univ.* **1990**, *11*, 135-142.
6. Berridge, M.J.; Lipp, P.; Bootman, M.D. The versatility and universality of calcium signalling. *Nat. Rev. Mol. Cell. Biol.* **2000**, *1*, 11-21.
7. Sanchez, J.C.; Wilkins, J.R. Changes in intracellular calcium concentration in response to hypertonicity in bovine articular chondrocytes. *Comp. Biochem. Physiol.* **2004**, *A137*, 173-182.
8. Pretorius, E.; Bornman, M.S. Calcium-mediated apoptosis plays a central role in the pathogenesis of estrogenic chemical-induced neurotoxicity. *Med. Hypotheses* **2005**, *65*, 893-904.
9. Alfonso, A.; Cabado, A.G.; Vieytes, M.R.; Botana, L.M. Calcium-pH crosstalks in rat mast cells: Cytosolic alkalinization, but not intracellular calcium release, is a sufficient signal for degranulation. *Br. J. Pharmacol.* **2000**, *130*, 1809-1816.
10. Lee, C.H.; Cragoe, E.J.J.; Edwards, A.M. Control of hepatocyte DNA synthesis by intracellular pH and its role in the action of tumor promoters. *J. Cell. Physiol.* **2003**, *195*, 61-69.
11. Kim, H.S.; Lee, Y.S.; Kim, D.K. Doxorubicin exerts cytotoxic effects through cell cycle arrest and Fas-mediated cell death. *Pharmacology* **2009**, *84*, 300-309.
12. Caterina, M.J.; Schumacher, M.A.; Tominaga, M.; Rosen, T.A.; Levin, J.D.; Julius, D. The capsaicin receptor: a heat-activated ion channel in the pain pathway. *Nature* **1997**, *389*, 816-824.
13. Shrode, L.D.; Tapper, H.; Grinstein, S. Role of intracellular pH in proliferation, transformation, and apoptosis. *J. Bioenerg. Biomembr.* **1997**, *29*, 393-399.
14. Deitmer, J.W.; Rose, C.R. pH regulation and proton signaling by glial-cells. *Progr. Neurobiol.* **1996**, *48*, 73-103.
15. Schwiening, C.J.; Willoughby, D. Depolarization-induced pH microdomains and their relationship to calcium transients in isolated snail neurones. *J. Physiol.* **2002**, *538*, 371-382.
16. Nitschke, R.; Riedel, A.; Ricken, S.; Leipziger, J.; Benning, N.; Fischer, K.G.; Greger, R. The effect of intracellular pH on cytosolic Ca²⁺ in HT29 cells. *Pflügers. Arch. Eur. J. Physiol.* **1996**, *433*, 98-108.
17. Salehzadeh, A.; Akhkha, A.; Cushley, W.; Adams, R.L.P.; Kusel, J.R.; Strang, R.H.C. The antimitotic effect of the neem terpenoid azadirachtin on cultured insect cells. *Insect Biochem. Mol. Biol.* **2003**, *33*, 681-689.

18. Huang, X.Y.; Li, O.W.; Xu, H.H. Induction of programmed death and cytoskeletal damage on Trichoplusiani BTI-Tn-5B1-4 cells by azadirachtin. *Pestic. Biochem. Phys.* **2010**, *98*, 289-295.
19. Salehzadeh, A.; Akhkha, A.; Cushley, W.; Adams, R.L.P.; Kusel, J.R.; Strang, R.H.C. The antimitotic effect of the neem terpenoid azadirachtin on cultured insect cells. *Insect Biochem. Mol. Biol.* **2003**, *33*, 681-689
20. Berridge, M.J. Neuronal calcium signaling. *Neuron* **1998**, *21*, 13-26.
21. Dupont, G.; Goldbeter, A. Properties of intracellular Ca^{2+} waves generated by a model based on Ca^{2+} -induced Ca^{2+} release. *Biophys. J.* **1994**, *67*, 2191-2204.
22. Li, X.Q.; Sun, J.H.; Yu, N.; Sun, Y.R.; Tan, Z.L.; Jiang, S.Q.; Li, N.; Zhou, C.X. Glutamate induced modulation of free Ca^{2+} in isolated inner hair cells of the guinea pig cochlea. *Chin. J. Otorhinolaryngol.* **2001**, *36*, 101-104.
23. Schwiening, C.J.; Kennedy, H.J.; Thomas, R.C. Calcium-hydrogen exchange by the plasma membrane Ca^{2+} -ATPase of voltage-clamped snail neurons. *Proc. Roy. Soc. B-Biol. Sci.* **1993**, *253*, 285-289.
24. Volk, T.; Hensel, M.; Kox, W.J. Transient Ca^{2+} changes in endothelial cells induced by low doses of reactive oxygen species: Role of hydrogen peroxide. *Mol. Cell. Biochem.* **1997**, *171*, 11-21.
25. Berridge, M. J. Calcium microdomains: organization and function. *Cell Calcium* **2006**, *40*, 405-412.
26. Rizzuto, R.; Marchi, S.; Bonora, M.; Aguiari, P.; Bononi, A.; De Stefani D.; Giorgi, C.; Leo, S.; Rimessi, A.; Siviero, R.; Zecchini, E.; Pinton, P. Ca^{2+} transfer from the ER to mitochondria: when, how and why. *Biochim. Biophys. Acta* **2009**, *1787*, 1342-1351.
27. Liao, W.C.; Huang, C.C.; Lu, Y.C.; Chi, C.C.; Chu, S.T.; Su, H.H.; Kuo, C.C.; Cheng, J.S.; Tseng, L.L.; Ho, C.M.; *et al.* Maprotiline-induced Ca^{2+} fluxes and apoptosis in human osteosarcoma cells. *Drug Develop. Res.* **2010**, *71*, 268-274.
28. Wang, Y.; Lin, J.S.; Wang, F.X. Calcium-mediated mitochondrial permeability transition involved in hydrogen peroxide-induced apoptosis in tobacco protoplasts. *J. Integr. Plant Biol.* **2006**, *48*, 433-439.
29. Michael, W. Calcium microdomains and cell cycle control. *Cell Calcium* **2006**, *40*, 585-592.
30. Takuwa, N.; Zhou, W.; Kumada, M.; Takuwa, Y. Ca^{2+} dependent stimulation of retino blastoma gene product phosphorylation and p34cdc2 kinase activation in serum stimulated human fibroblasts. *J. Biol. Chem.* **1993**, *268*, 138-145.
31. Parry, H.D.; McDougall, A.D.; Whitaker, M. Microdomains bounded by endoplasmic reticulum segregate cell cycle calcium transients in syncytial *Drosophila* embryos. *J. Cell. Biol.* **2005**, *171*, 47-59.
32. Parry, H.D.; McDougall, A.D.; Whitaker, M. Endoplasmic reticulum generates calcium signalling microdomains around the nucleus and spindle in syncytial *Drosophila* embryos. *Biochem. Soc. Transact.* **2006**, *34*, 385-388.
33. FitzHarris, G.; Larman, M.; Richards, C.; Carroll, J. An increase in $[\text{Ca}^{2+}]_i$ is sufficient but not necessary for driving mitosis in early mouse embryos. *J. Cell Sci.* **2005**, *118*, 4563-4575.
34. Jana, S.; Jana, O.; Monika, L.; Lucie, R.; Zdeněk, K.; Miroslav, S. Brassinosteroids cause cell cycle arrest and apoptosis of human breast cancer cells. *Chem.-Biol Interact.* **2010**, *188*, 487-496.

35. Lohr, C.; Rose, C.R.; Deitmer, J.W. Extracellular Ca^{2+} changes during transmitter application in the leech central nervous system. *Neurosci. Lett.* **1996**, *205*, 57-60.
36. Glitsch, M.G.; Bakowski, D.; Parekh, A.B. Store-operated Ca^{2+} entry depends on mitochondrial Ca^{2+} uptake. *EMBO J.* **2002**, *21*, 6744-6754.
37. Brustovetsky, N.; Dubinsky, J.M. Dual responses of CNS mitochondria to elevated calcium. *J. Neurosci.* **2000**, *20*, 103-113.
38. Snowdowne, K.W.; Way, B.; Thomas, G.; Chen, H.Y.; Cashman, J.R. pHi controls cytoplasmic calcium in rat parotid cells. *Biochim. Biophys. Acta* **1992**, *1108*, 145-152.
39. Kaila, K.; Voipio, J. Dependence of intracellular free calcium and tension on membrane potential and intracellular pH in single crayfish muscle fibres. *Pflügers. Arch. Eur. J. Physiol.* **1990**, *416*, 501-511.
40. Sedova, M.; Blatter, L.A. Intracellular sodium modulates mitochondrial calcium signaling in vascular endothelial cells. *J. Biol. Chem.* **2000**, *275*, 35402-35407.
41. Kao, J.P.Y. Practical aspects of measuring $[\text{Ca}^{2+}]$ with fluorescent indicators. *Methods Cell Biol.* **1994**, *40*, 155-181.

Sample Availability: Rhodojaponin-III is available from the authors.

© 2011 by the authors; licensee MDPI, Basel, Switzerland. This article is an open access article distributed under the terms and conditions of the Creative Commons Attribution license (<http://creativecommons.org/licenses/by/3.0/>)